*36th EPS Conference on Plasma Phys. Sofia, June 29 - July 3, 2009 ECA Vol.**33E**, P-4.136 (2009)*

Influence of Magnetic Field Inhomogeneity on Electron Cyclotron Power Losses in Magnetic Fusion Reactor

A.B. Kukushkin[a], P.V. Minashin[a,b]

[a] *Nuclear Fusion Institute, RRC "Kurchatov Institute", Moscow 123182, Russia*

[b] *Moscow Engineering Physics Institute, Moscow 115409, Russia*

1. Introduction. Recent comparison [1] of numeric codes SNECTR [2], CYTRAN [3], CYNEQ [4], and EXACTEC [5] for calculating the 1D distribution, over magnetic flux surfaces, of the net electron cyclotron (EC) wave power density, $P_{EC}(\rho)$, emitted for different electron temperature profiles and average temperatures of relevance for fusion reactor-grade magnetoplasmas, was carried out for *homogeneous* profile of *total* magnetic field, averaged over magnetic flux surface: $B(\rho)=const=B_T(R_0)$ (e.g., for ITER "inductive" regime the profile $B(\rho)$ is flat with accuracy ~20% [6]). The comparison [1] was carried out in view of the potential importance of EC wave emission in the local electron power balance for ITER and tokamak-reactor steady-state operation [7].

Here we analyze the influence of the *inhomogeneity* of total magnetic field profile on the $P_{EC}(\rho)$ profile, spectral intensity of outgoing radiation, and total (i.e. volume-integrated) power losses.

2. Comparison of EC power losses for three representations of total magnetic field.

Total magnetic field in the plasma column calculated as a sum of toroidal field, with account of Shafranov shift, and poloidal field, may be represented as (i) 2D profile of magnetic field, $B(\rho,\theta)$, as a function of magnetic flux surface variable ρ (square root of normalized toroidal magnetic flux) and poloidal angle θ; (ii) 1D profile $B(\rho)$, calculated by averaging $B(\rho,\theta)$ over θ; (iii) flat profile, $B(\rho)=const= B_T(R_0)\equiv B_0$ – vacuum toroidal field on axis. Here, 2D magnetic field is calculated, taking an approximation of elliptic form of nested magnetic surfaces (Fig. 3), and its 1D version is compared with that from ASTRA modeling [8] (Fig. 4).

We made a comparison of calculations with the modified code CYNEQ for above three representations of total magnetic field profile, and density and temperature profiles, shown in Fig. 1, and other parameters taken close to ITER case: major radius $R_0 = 6.20$ м, minor radius a =1.85 м, elongation k= 1.97, B_0 = 5.3 T, effective coefficient of EC wave reflection from the wall R_w= 0.6 (see Figs. 4,5). Note that the increase of the net absorption (i.e. modulus of $P_{EC}(\rho)$) in the peripheral plasma for $B(\rho,\theta)$ case relative to $B(\rho)$ and B_0

cases is to be examined with further modification of the code CYNEQ (one should decouple magnetic flux surfaces from surfaces [3,4] of a constant optical depth, counted from the plasma edge).

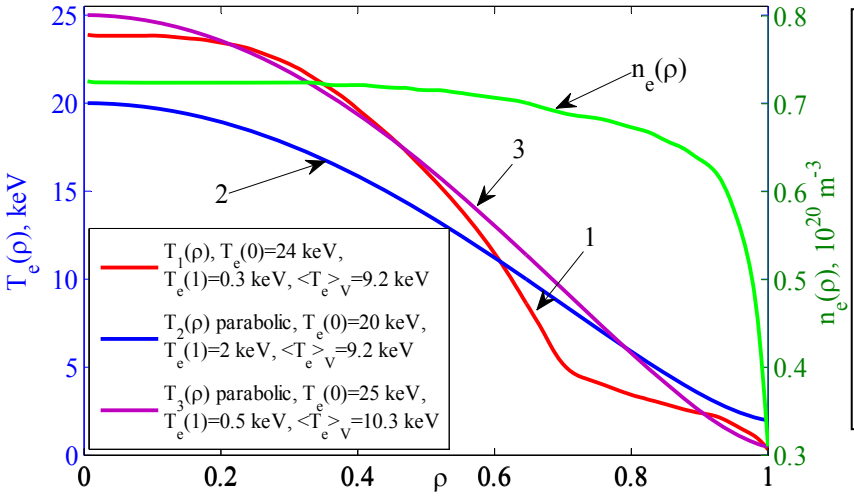

Fig. 1. Electron temperature and density profiles: (1) – T_e (and n_e) data [8] of ASTRA code modeling of ITER scenario 4; (2) – parabolic T_e profile with a pedestal, with the same volume-average temperature as in the case 1; (3) - parabolic T_e profile with a slightly higher central and edge temperatures than in the case 1.

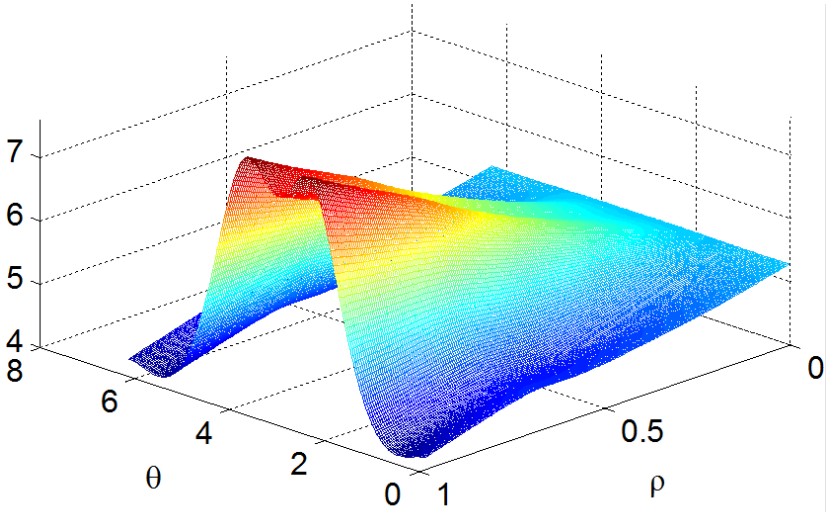

Fig. 2. The 2D profile of total magnetic field B(ρ,θ) (in Tesla), calculated as a sum of toroidal field, with account of Shafranov shift (Fig.3), and poloidal field, calculated from safety factor (Fig.3) in cylindrical approximation.

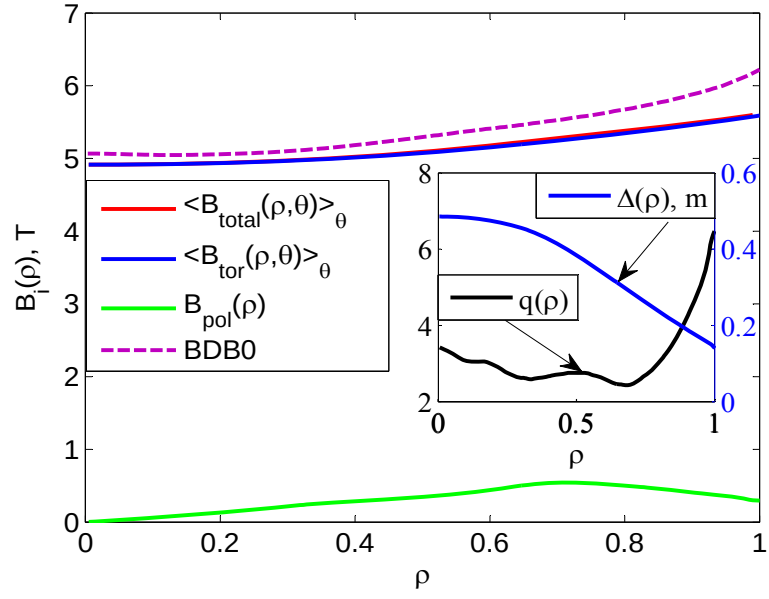

Fig. 3. The 1D profiles of toroidal, poloidal and total magnetic field, calculated from 2D field in Fig 2 (solid curves), and 1D total magnetic field from ASTRA data [8] (curve BDB0). Inserts: Profiles of safety factor, q(ρ), and Shafranov shift, Δ(ρ), taken from data [8] of ASTRA code modeling of ITER scenario 4.

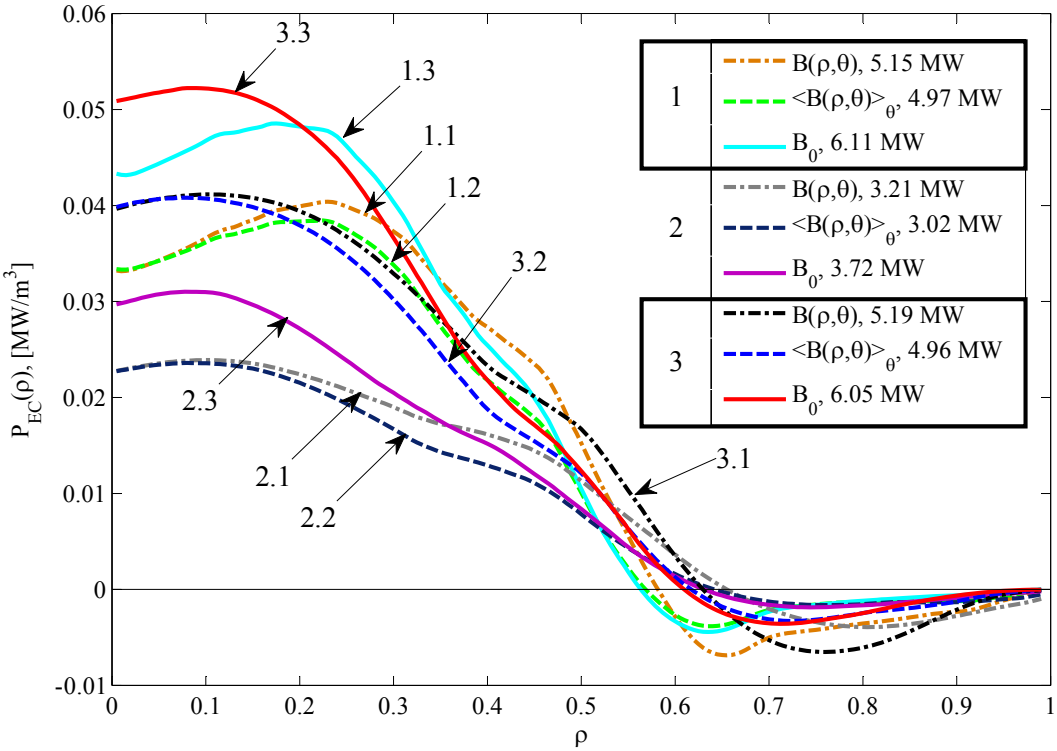

Fig. 4. Profiles of power density loss, $P_{EC}(\rho)$, calculated with modified code CYNEQ for three cases of electron temperature (indicated with first number in curve numbering, according to Figure 1) and the following three cases of total magnetic field (indicated with second number in curve numbering): (1) 2D total magnetic field $B(\rho,\theta)$ (boundaries of optically thin outer layer [3,4] are calculated for $B(\rho)$ profile, absorption and emission are calculated for $B=B(\rho,\theta)$ and are averaged over magnetic surface), (2) 1D total magnetic field $B(\rho)$ (absorption and emission are calculated for $B=B(\rho)$), (3) constant magnetic field, which is equal to vacuum toroidal magnetic field on the axis, $B=B_0$. The respective total power losses, calculated by integration of $P_{EC}(\rho)$ over plasma volume, are indicated.

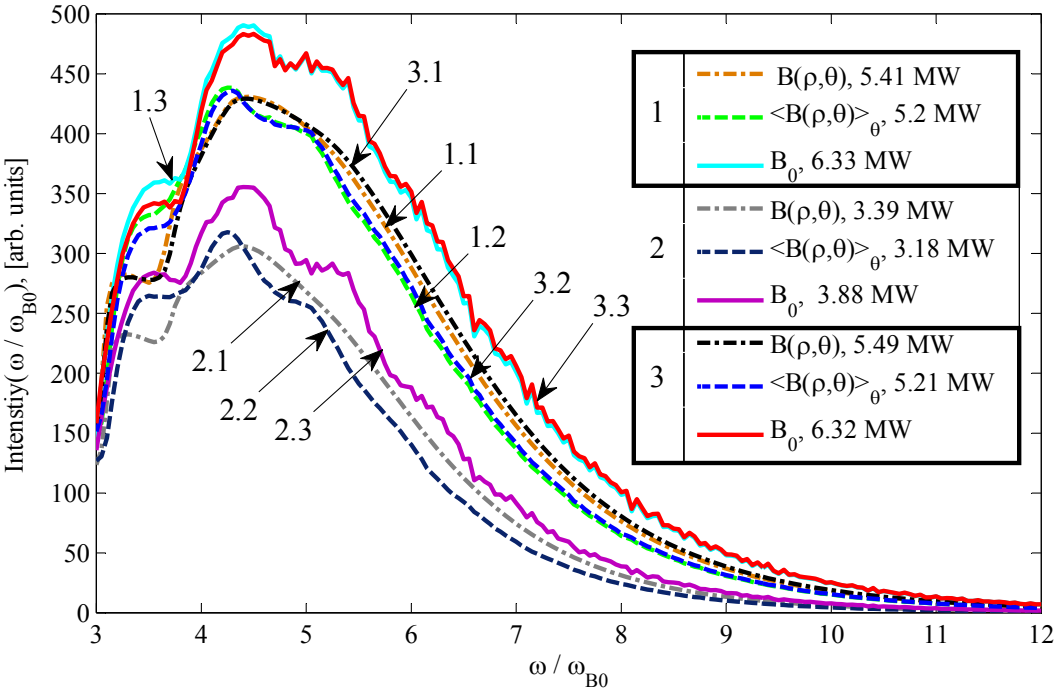

Fig. 5. Spectral intensity of outgoing radiation (in units of fundamental gyrofrequency for vacuum toroidal field on the axis, B_0) for the cases of Fig. 4. The respective total power losses, calculated by integration over frequency, are indicated.

The accuracy of using our approximation of 2D and 1D magnetic field profiles in calculating the $P_{EC}(\rho)$ profile, is illustrated with Figs. 6,7.

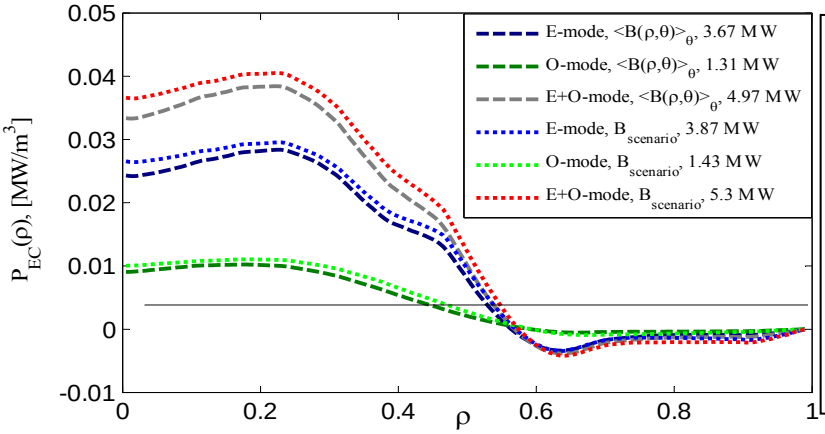

Fig. 6. Comparison of profiles of power density loss, $P_{EC}(\rho)$, calculated for two profiles of 1D total magnetic field $B(\rho)$: (i) calculated by averaging 2D magnetic field $B(\rho,\theta)$ in Fig. 2, and (ii) ASTRA data BDB0 [8]. Also the contributions of each EC wave mode and total power losses, calculated by integration of $P_{EC}(\rho)$ over plasma volume, are indicated.

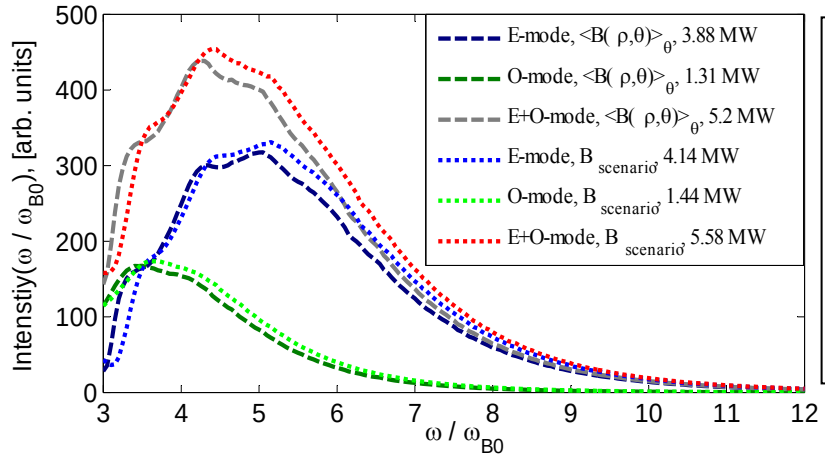

Fig. 7. Comparison of intensities of outgoing radiation (and total power losses) for the cases of Fig. 6. Also the contributions of each EC wave mode and total power losses, calculated by integration over frequency, are indicated.

3. Conclusions. Main result of our comparison is that the profile of EC power density losses, $P_{EC}(\rho)$, calculated for $B(\rho,\theta)$ and $B(\rho)$ profiles of total magnetic field is lower than that for $B=B_0$ by $\sim<$ 25% in the central plasma, with the respective decrease of total (volume-integrated) losses being lower by $\sim<$20%. This is due to a decrease of both $B(\rho,\theta)$ and $B(\rho)$ in the center, with respect to B_0, because of Shafranov shift.

Acknowledgements. The authors are grateful to A.Yu. Dnestrovskii and A.R. Polevoi for helpful discussions.

REFERENCES

[1] Albajar F., Bornatici M., Engelmann F., Kukushkin A.B., Fusion Sci. & Technol., **55**, 76-83 (2009).
[2] Tamor S., Nucl. Technol. Fusion, **3**, 293 (1983).
[3] Tamor S., Report SAI-023-81-189-LJ/LAPS-72 (La Jolla, CA: Science Applications), 1981.
[4] Kukushkin A.B., Proc. 14th IAEA Conf. on Plasma Phys. and Contr. Fusion, 1992, v.2, pp. 35-45; Cherepanov K.V., Kukushkin A.B., Proc. 20th IAEA Fusion Energy Conf. (Vilamoura, 2004), TH/P6-56.
[5] Albajar F., Bornatici M., Engelmann F., Nucl. Fusion, **42**, 670 (2002).
[6] Polevoi A.R., Medvedev S.Yu., Mukhovatov S.V., *et. al.*, J Plasma Fusion Res. SERIES, **5,** 82-87 (2002).
[7] Albajar F., *et al.*, Nucl. Fusion, **45**, 642 (2005).
[8] Polevoi A.R., *et al.*, Proc. 19th IAEA Conf. on Fusion Energy (Lyon, 2002) CT/P-08.